frontiers | Frontiers in Astronomy and Space Sciences

TYPE Review
PUBLISHED 24 July 2025
DOI 10.3389/fspas.2025.1587415

OPEN ACCESS

EDITED BY
Maurizio Maria Busso,
University of Perugia, Italy

REVIEWED BY
Sara Palmerini,
University of Perugia, Italy
Lili Wang,
Dezhou University, China

*CORRESPONDENCE
Yin-Bi Li,
ybli@bao.ac.cn
A-Li Luo,
lal@nao.cas.cn

RECEIVED 04 March 2025
ACCEPTED 16 June 2025
PUBLISHED 24 July 2025

CITATION
Lu H-L, Li Y-B, Luo A-L, Zou Z-Q, Kong X-M, Yi Z-P, Jones HRA, Liang J-C and Li S (2025) A review of the search for AGB stars.
Front. Astron. Space Sci. 12:1587415.
doi: 10.3389/fspas.2025.1587415

A review of the search for AGB stars

Hai-Ling Lu [1,2], Yin-Bi Li [1]*, A-Li Luo [1,2,3]*, Zhi-Qiang Zou [4,5,6], Xiao-Ming Kong [7], Zhen-Ping Yi [7], Hugh R. A. Jones [8], Jun-Chao Liang [1,2] and Shuo Li [1,2]

[1]CAS Key Laboratory of Optical Astronomy, National Astronomical Observatories, Chinese Academy of Sciences, Beijing, China, [2]University of Chinese Academy of Sciences, Beijing, China, [3]School of Information Management and Institute for Astronomical Science, Dezhou University, Dezhou, China, [4]College of Computer, Nanjing University of Posts and Telecommunications, Nanjing, China, [5]Jiangsu Key Laboratory of Big Data Security and Intelligent Processing, Nanjing, China, [6]University of Chinese Academy of Sciences, Nanjing, China, [7]School of Mechanical, Electrical and Information Engineering, Shandong University, Weihai, China, [8]School of Physics, Astronomy and Mathematics, University of Hertfordshire, Hatfield, United Kingdom

The Asymptotic Giant Branch (AGB) is the late stage of the evolution of intermediate and low-mass stars and is of great importance for understanding stellar evolution, nucleosynthesis, and the chemical evolution of galaxies. This paper systematically reviews the methods for identifying AGB stars, from both traditional approaches and machine learning techniques. By integrating multi-wavelength data such as optical and infrared spectra, along with stellar evolution models, we analyze the existing methods and potential directions for improvement. We also explore the possibility of using interpretable machine learning algorithms to discover new features and applying deep learning algorithms to enhance search efficiency. With the advancement of data processing technology and the widespread application of machine learning methods, future AGB star searches will be more accurate and efficient. The increased number of discoveries, enabled by more advanced search methods, will particularly enhance our ability to reveal examples of short-lived late-stage stellar evolutionary processes.

KEYWORDS

asymptotic giant branch stars, late-type stars, stars evolution, Hertzsprung–Russell and colour–magnitude diagrams, machine learning

1 Introduction

The Asymptotic Giant Branch (AGB) is a region in the Hertzsprung-Russell diagram characterized by low temperature and high luminosity, representing a stage in the late evolution of all low-to intermediate-mass stars (approximately 0.8–8 $M_{\odot}$) (Höfner and Olofsson, 2018; Nowotny et al., 2001). At this stage, the stellar core is composed of carbon and oxygen, while the hydrogen and helium shells undergo burning surrounding the carbon-oxygen core. The s-process during the AGB phase produces heavier elements, which, along with carbon, are mixed into the outer envelope during the third dredge-up process. These elements are then released into the interstellar medium through strong stellar winds.

As a result, AGB stars are crucial for understanding stellar evolution, elemental abundance, and chemical evolution within the Milky Way. Additionally, before removing their outer layers to form planetary nebulae and evolving into white dwarfs, AGB stars experience significant mass loss, providing a valuable opportunity to study the

formation of interstellar dust and molecular gas (Habing and Olofsson, 2004; Herwig, 2005). As one of the primary contributors to the recycling of interstellar material, the mass loss process of AGB stars also has a profound impact on the chemical enrichment, dynamics, and structural evolution of the surrounding interstellar medium (Iben and Renzini, 1983). Therefore, the search and study of AGB stars hold a crucial position in the field of astronomy and they serve as a key component in the chemical evolution of galaxies.

AGB stars can be classified in various ways based on their evolutionary stage, surface chemical composition, and variability period. The AGB phase can be divided into the Early Asymptotic Giant Branch (E-AGB) phase and the Thermally Pulsing Asymptotic Giant Branch (TP-AGB) phase. Initially during the E-AGB phase, the helium shell undergoes stable nuclear fusion, and the stellar core consists of inert carbon and oxygen. Over time, the star enters the TP-AGB phase, where it experiences periodic thermal pulses, meaning the helium shell ignites convectively in periodic thermal instabilities, causing significant fluctuations in both the star's luminosity and mass loss rate (Herwig, 2005). During the TP-AGB phase, the nucleosynthesis process coupled with mixing episodes leads to significant changes in surface chemical composition, especially an increase in carbon content, with AGB stars within a certain mass range evolving into carbon stars at this stage. Moreover, the large-scale mass loss during the TP-AGB phase ultimately determines whether the star can form a planetary nebula and evolve into a white dwarf (Vassiliadis and Wood, 1993).

Another common basis for classification is the surface chemical composition, which mainly divides AGB stars into oxygen-rich AGB stars (O-rich AGB) and carbon-rich AGB stars (C-rich AGB). Oxygen-rich AGB stars, whose spectral types include M-type and S-type, are characterized by a C/O ratio less than 1, with TiO as their primary molecular absorption line; these stars are usually in the earlier stages of AGB evolution (Willson, 2000). As the nucleosynthesis processes proceed, stars of about 2–3 $M_{\odot}$ gradually evolve into carbon-rich stars, whose spectral type is classified as C-type, and they are characterized by a C/O ratio greater than 1. Their main absorption lines are carbon-based molecules such as C_2 and CN, and these stars are typically in the later stages of AGB evolution.

AGB stars can also be classified based on their photometric periods. As soon as stars enter the TP-AGB phase,the majority of them exhibit variability in their luminosity due to thermal pulses. These variable stars are further divided into Mira variables, Semi-Regular Variables (SRVs), and Irregular variables. The distinctive features are the regularity of light curves, their amplitude and their period (Ivezić and Knapp, 1999; Soszyński et al., 2013; Bhardwaj et al., 2019).

Methods for searching for AGB stars have evolved progressively from traditional manual feature construction to modern machine learning algorithms. Traditional approaches primarily rely on astronomers' expertise, identifying AGB stars through specific features such as spectral characteristics and photometric variability (Lebzelter et al., 2023; Li et al., 2024). In the optical wavelength range, the low surface temperatures of AGB stars cause their spectra to exhibit prominent absorption lines of oxide molecules (e.g., TiO and VO) or carbon-based molecules (e.g., C_2 and CN). These features are used to distinguish oxygen-rich AGB stars from carbon-rich stars (Habing and Olofsson, 2004).

Infrared search methods are also particularly important because AGB stars form extensive dust shells due to intense mass loss, leading to significantly enhanced infrared emission. Consequently, infrared survey projects such as 2MASS (Two Micron All Sky Survey) and WISE (Wide-field Infrared Survey Explorer) have become essential resources for identifying AGB stars (Cutri et al., 2003; Wright et al., 2010). Similarly, sub-millimeter and radio observations provide a route to penetrate obscuration using molecular lines and masers. Observations in the radio band primarily rely on molecular gases produced during the mass-loss processes of AGB stars, such as OH molecular lines (Khouri et al., 2019), or masers like OH, H_2O and SiO masers (Baud et al., 1979; Deacon et al., 2007; Kim et al., 2010; Stroh et al., 2019).

Additionally, since AGB stars are typically variable, they can be effectively identified through the characteristics of their light curves. Survey projects such as OGLE (Optical Gravitational Lensing Experiment) and ASAS-SN (All-Sky Automated Survey for Supernovae) have extensively utilized this identification method in their searches (Soszyński et al., 2013; Jayasinghe et al., 2019).

With the growth of data volume and the rapid advancement of computer technology, machine learning has gradually become an effective tool for searching AGB stars. Compared to traditional methods of manual feature extraction and visual inspection, machine learning enables the identification of complex patterns in high-dimensional survey data such as spectra. Researchers have employed various machine learning techniques, including Support Vector Machines (SVM), XGBoost, and Convolutional Neural Networks (CNNs), among others (Si et al., 2014; Si et al., 2015; Li et al., 2018; Chen et al., 2022; Chen et al., 2023; He et al., 2024; Ye et al., 2025; Roulston et al., 2025), to classify AGB stars with greater accuracy. These methods have been especially effective in identifying carbon-rich (C-type) and S-type AGB stars, which exhibit characteristic molecular bands (e.g., C_2, CN, or ZrO) in their spectra. For example, SVM and ensemble methods (like XGBoost) have been used to distinguish S-type stars based on ZrO band indices (Chen et al., 2022; Chen et al., 2023), while CNN-based models have achieved high accuracy in classifying carbon stars from large spectroscopic datasets (He et al., 2024; Ye et al., 2025). However, due to the spectral overlap between oxygen-rich AGB stars and other red giants, current machine learning applications for O-rich AGB identification remain limited. Expanding the use of interpretable algorithms and multimodal data fusion is expected to further enhance the efficiency and precision of machine learning in AGB star searches.

2 Characteristics of AGB stars

Observationally, AGB stars appear as bright red giants, with luminosities reaching several thousand times that of the Sun.

2.1 Structure and evolution of AGB stars

An AGB star can be described as consisting of six parts (see Figure 1): (i) a degenerate C/O core, (ii) a He burning shell, (iii) a H burning shell, (iv) a large and cold convective stellar

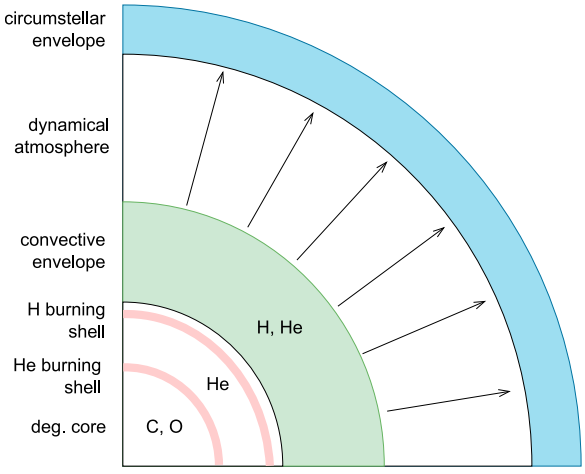

FIGURE 1
Schematic structure of an AGB star during its thermally pulsing phase.

envelope, (v) a tenuous dynamical atmosphere, and (vi) a very large, very diluted, and cold circumstellar envelope.

Thus, an AGB star covers more than 10 orders of magnitude in size scale, 30 orders of magnitude in density scale, and seven orders of magnitude in temperature scale. Specifically, the temperature range of AGB stars is approximately 10 K to 10^8 K, with the temperature gradually decreasing from the inside to the outside. The temperature of the He-burning region is about 10^8 K, while the temperature of the outermost circumstellar envelope is below 10 K (e.g., Habing and Olofsson, 2004; Li et al., 2014; Li et al., 2016).

The evolution of the AGB phase can be broadly divided into two stages: E-AGB and TP-AGB. During the E-AGB phase, the helium shell burns while the hydrogen shell is extinguished. Toward the end of the E-AGB phase, the hydrogen shell contracts and heats up until it reignites. As the intershell region accumulates additional helium produced by the hydrogen-burning shell above, the He shell reaches the conditions necessary for unstable ignition. This marks the onset of the TP-AGB phase, characterized by the thermally unstable He-burning shell undergoing periodic thermal pulses. After the onset of the TP-AGB phase, as helium shell burning proceeds, the He-rich intershell region expands, causing the temperature in the hydrogen shell to decrease and hydrogen burning to be extinguished. Expansion and cooling of the intershell region can also lead to a deeper penetration of the outer convective envelope. In some cases, convection can penetrate beyond the now extinct H-burning shell, such that material from the intershell region is mixed into the outer envelope. This phenomenon is called third dredge-up (TDU). Then, as the star contracts again under gravity, the hydrogen shell region heats up, hydrogen burning restarts and the He-burning shell becomes inactive. A long phase of stable H-shell burning follows in which the mass of the intershell region grows until the next thermal pulse occurs.

During the TP-AGB phase, the third dredge-up episode mixes carbon from the intershell region into the stellar envelope. Whether an AGB star evolves into a carbon star depends on several factors, including metallicity, initial stellar mass, mass loss rate, the dredge-up efficiency, the occurrence of Hot Bottom Burning (HBB), and extra mixing (e.g., Stancliffe et al., 2004; Cristallo et al., 2009; Palmerini et al., 2011; Karakas, 2014). For example, both sufficient thermal pulses and adequate dredge-up efficiency (λ) are required to accumulate enough carbon for the C/O ratio to exceed 1, since λ typically increases with successive pulses (Stancliffe et al., 2004). The ^{12}C-enrichment by TDU is partly compensated by its destruction in extra-mixing processing during the interpulse stages (Palmerini et al., 2011). In addition, a sudden massive ejection event may terminate the AGB phase of the central source in advance, preventing its transformation into a carbon star (Masa et al., 2024).

The third dredge-up also brings elements synthesized *via* the slow neutron-capture process (s-process) into the stellar envelope. In the AGB stars the s-process occurs in the He rich layers of the stars, during both the interpulse period (the H-shell is burning) thanks to the neutrons delivered by the ^{13}C $(\alpha,n)^{16}$O reaction and the thermal pulses thanks to the neutrons from ^{22}Ne $(\alpha,n)^{25}$Mg. In the most of the AGBs the ^{13}C $(\alpha,n)^{16}$O is the main source of neutrons for the s-process. These neutrons are captured by seed nuclei, producing heavier elements through a sequence of slow neutron captures and β-decays. Typical s-process elements include light-s elements such as Sr, Y, and Zr, as well as heavy-s elements such as Ba, La, and Pb. This nucleosynthetic pathway is a hallmark of AGB stars confirmed by Lambert et al. (1995). The TP-AGB phase is characterized by the simultaneous action of internal nucleosynthesis, convective mixing and a strong stellar wind. This leads to them to significantly contribute to the chemical enrichment of galaxies as well as up to 40 per cent of interstellar medium dust (e.g., Schneider et al., 2014; Goldman et al., 2022).

2.2 Observational characteristics of AGB stars

Features in the optical band. AGB stars are classified based on the C/O ratio in their atmospheres, with oxygen-rich AGB stars having C/O < 1 and carbon-rich AGB stars having C/O > 1. Alternatively, they can be classified by spectral type (Ramstedt et al., 2011; Shetye et al., 2019): M-type (C/O < 0.5), S-type (0.5 < C/O < 1), C-type (C/O > 1), and the intermediate MS and SC type. Optical observational characteristics of AGB stars include: M-type stars have spectra dominated by TiO molecular bands (and VO for very cool stars); the spectra of S-type stars are characterized by enhanced bands of molecules involving s-process elements (like Sr, Y, Zr, Ba, La, Ce, Nd, Sm, Tc, and Pb), such as ZrO, YO and LaO (Herwig, 2005); and C-type stars have spectra dominated by C_2 and CN molecular bands (as shown in Figure 2). The MS type is a transitional type between M-type and S-type stars, containing strong YO, TiO and weak ZrO molecules, while the SC type is a transitional type between S-type and C-type stars, containing weak ZrO, C_2, and strong Na I D-lines (Keenan and Boeshaar, 1980; Gray and Corbally, 2009; Van Eck et al., 2017). In addition, recent studies suggest that a small number of S-type stars also exhibit the CN characteristics of C-type stars. The possible reason is that the external ultraviolet radiation field of these stars may, in certain cases, effectively promote the photodissociation of HCN, thereby increasing the abundance of CN (Feng et al., 2024).

Molecular line features in the infrared and radio band. In the infrared band, O-rich AGB stars exhibit oxygen-rich molecular

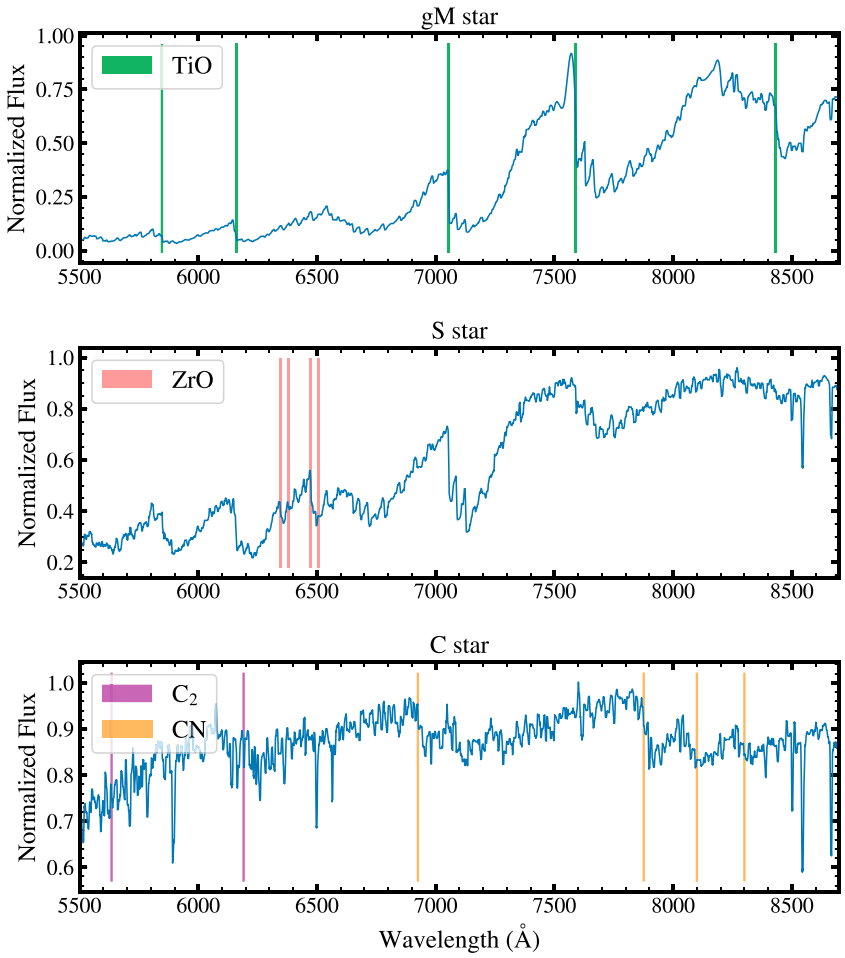

FIGURE 2
Spectra of M giants, S-type stars, and carbon stars from the LAMOST low-resolution spectral library, with their characteristic molecular bands indicated in the figure.

bands such as SiO, SiO_2 and H_2O, while C-rich AGB stars display carbon-rich molecular bands such as C_2H_2 and HCN (Waters et al., 1999) (as shown in Figure 3). In the radio band, common molecular spectral lines in C-rich AGB stars include C_2H, C_4H, HC_3N (Tuo et al., 2024). And in O-rich AGB stars, the main molecular lines are OH lines (Khouri et al., 2019).

Dust features. Oxygen-rich AGB stars with amorphous silicate in the dust envelop exhibit either absorption or emission features at around 10 and 18 μm, depending on the optical depth and mass-loss rate (Sylvester et al., 1999; Engels, 2005). In contrast, carbon-rich AGB stars typically show an emission feature near 11.3 μm, which is attributed to silicon carbide (SiC) dust grains (Gobrecht et al., 2017; Suh, 2021) (as shown in Figure 4).

Masers features. Masers in the circumstellar envelopes of oxygen-rich stars include OH masers at 1612, 1665 and 1667 MHz (Engels and Bunzel, 2015), H_2O masers at 22 GHz (Wu et al., 2022), and SiO masers at 43 and 86 GHz (Stroh et al., 2018). Masers in the circumstellar envelopes of carbon-rich stars include HCN and SiS masers (Fonfría Expósito et al., 2006; Menten et al., 2018; Bhardwaj et al., 2019).

Variability features. The TP-AGB phase is characterized by variability in brightness. Mira stars are a type of prominent variable stars located in the TP-AGB phase, and their light curves have obvious features of large amplitudes ($\Delta V \gtrsim 2.5$ mag, $\Delta I \gtrsim 0.8$ mag, $\Delta K \gtrsim 0.4$ mag, and $\Delta[3.6] \gtrsim 0.2$ mag) and long periods (~100–1000 days) (Bhardwaj et al., 2019). Semi-Regular Variables display some degree of periodicity in their luminosity variations but are less regular than Mira variables, and their amplitudes are smaller, with I-band amplitude $\Delta I < 0.8$ mag (Soszyński et al., 2009; 2013). Irregular variables, on the other hand, show no obvious periodicity in their luminosity variations, with inconsistent variation amplitudes (Ivezić and Knapp, 1999; Jayasinghe et al., 2019).

3 Traditional methods for searching AGB stars

In practical observations and data analysis, the identification of AGB stars relies on various observational indicators and methods. Since AGB stars exhibit distinct characteristics in terms of spectral features, color, magnitude, and maser distribution, the search for AGB stars typically involves a multidimensional approach for comprehensive analysis. This section will discuss in detail the identification methods and current applications of AGB stars from

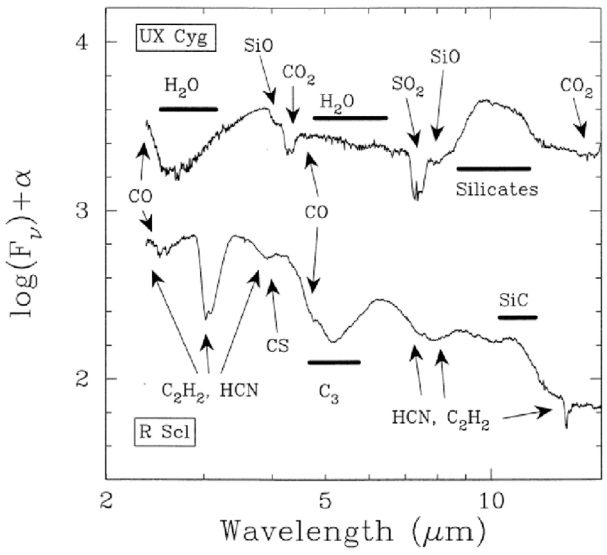

FIGURE 3
Examples of ISO-SWS spectra of AGB stars with modest mass loss rates, UX Cyg (top, O-rich), and R Scl (bottom, C-rich). The strongest molecular absorption bands are indicated. Picture reproduced from Waters et al. (1999) with permission from © ESA.

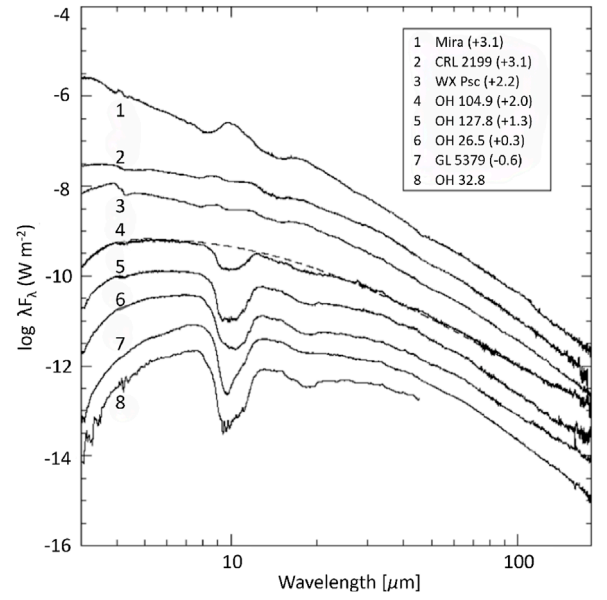

FIGURE 4
ISO spectra of several O-rich AGB stars in the 6–200 μm region are ordered by their 10 μm optical depth, with stars having higher mass loss rates generally showing deeper silicate absorption at 10 μm. Credit: Sylvester et al. (1999), A&A, 352, 587, reproduced with permission © ESO.

four perspectives: color and magnitude, light curves, infrared spectra, and radio masers. By utilizing different observational techniques, we can capture the prominent features of AGB stars across multiple wavelengths, thereby improving the identification rate and classification accuracy of AGB stars.

3.1 Search methods using color and magnitude criteria

Color-Color Diagrams and Color-Magnitude Diagrams are commonly used tools in astronomy for classifying and studying stellar types, and they are also applicable for identifying AGB stars. Among them, the color-magnitude diagram is essentially the observational version of the Hertzsprung-Russell diagram (HR diagram).

The color of a star is closely related to its surface temperature. Stars with higher temperatures emit more blue light, appearing bluer, while stars with lower temperatures appear redder. AGB stars are generally cooler stars with lower temperatures, so they are positioned redder on Color-Color Diagrams and Color-Magnitude Diagrams, showing a higher degree of redness. AGB stars are giant stars with large radii and high luminosities, so they are typically located in the high-luminosity, redder regions of the color-magnitude diagram.

The color-color diagrams or color-magnitude diagrams currently used to search for AGB stars are essentially linear separation methods. The commonly used color diagram methods are shown in Table 1.

For example, the (K_s-W3, J-K_s) color-color diagram based on WISE and 2MASS is shown in Figure 5 (Tu and Wang, 2013). The three zones that include most of the AGB stars in Figure 5 correspond to equations from Equations1–6:

For 0.35 < (K_s - W3) < 1.45:

$$(J-K_s) > 0.42 + 0.8 \times (K_s - W3), \quad (1)$$

$$(J-K_s) < 0.72 + 1.66 \times (K_s - W3), \quad (2)$$

for (K_s - W3) > 1.45:

$$(J-K_s) > 0.71 + 0.6 \times (K_s - W3), \quad (3)$$

$$(J-K_s) < 2.25 + 0.6 \times (K_s - W3), \quad (4)$$

and,

$$(J-K_s) > 1.29 + 0.2 \times (K_s - W3), \quad (5)$$

$$(J-K_s) < 0.71 + 0.6 \times (K_s - W3). \quad (6)$$

The (J-K_s, K_s) color-magnitude diagram based on 2MASS JHK photometry is shown in Figure 6 (Cioni et al., 2006a; b; Boyer et al., 2011).

The three solid lines in the figure correspond to Equations 7–9:

$$K_{s0} = -0.48 \times (J-K_s)_0 + 13, \quad (7)$$

$$K_{s0} = -13.333 \times (J-K_s)_0 + 24.666, \quad (8)$$

$$K_{s0} = -13.333 \times (J-K_s)_0 + 28.4. \quad (9)$$

TABLE 1 Traditional AGB star search methods based on color diagrams.

Data sources	Methods	References
2MASS/UKIRT		Cioni et al. (2006a)
		Cioni et al. (2006b)
		Groenewegen et al. (2009)
		Wiśniewski et al. (2011)
	(H-K, J-H) Color-Color Diagram	Nikolaev and Weinberg (2000)
	(J-K, K) Color-Magnitude Diagram	Boyer et al. (2011)
		Kacharov et al. (2012)
		Sibbons et al. (2015a)
		Sibbons et al. (2015b)
		Battinelli and Demers (2011)
DENIS	(J-K, I-J) Color-Color Diagram	Cioni and Habing (2003)
		Loup et al. (1998)
Strömgren	(b, b-y) Color-Magnitude Diagram	Gruyters et al. (2017)
	(y, v-y) Color-Magnitude Diagram	Campbell et al. (2013)
Subaru Suprime-Cam	(V-I, I)Color-Magnitude Diagram	Leščinskaitė et al. (2021)
CFHT V and I, TiO and CN filters	(V-I, I) Color-Magnitude Diagram	Brewer et al. (1995)
		Albert et al. (2000)
Du Pont R and I, TiO and CN filters	(R-I, CN-TiO) Color-Color Diagram	Nowotny et al. (2001)
NOT V and i, TiO and CN filters	(V-i/I, CN-TiO) Color-Color Diagram	Nowotny et al. (2002)
		Nowotny et al. (2003)
WISE	(W1-W2, W3-W4) Color-Color Diagram	Lian et al. (2014)
		Wu et al. (2018)
WISE and 2MASS	(J-Ks, Ks-W3) Color-Color Diagram	Suh (2021)
		Lian et al. (2014)
		Tu and Wang (2013)

(Continued on the following page)

TABLE 1 (*Continued*) Traditional AGB star search methods based on color diagrams.

Data sources	Methods	References
MSX and 2MASS	[A]-[D], [A]-[E] and [C]-[E] color index	Lewis et al. (2020b)
	(K-A, J-K) and (K-A, H-K) Color-Color Diagram	Lewis et al. (2020a)
		Kastner et al. (2008)
Spitzer IRAC/MIPS	([3.6]-[8.0], [8.0]) Color-Magnitude Diagram	Matsuura et al. (2009)
	([8.0]-[24], [5.8]-[8.0]) Color-Color Diagram	Blum et al. (2006)
Spitzer IRAC and 2MASS	(J-[3.6], [3.6]) Color-Magnitude Diagram	Spano et al. (2011)
		Srinivasan et al. (2009)
IRAS and/or 2MASS	([12]-[25], [25]-[60]) Color-Color Diagram	van der Veen and Habing (1988)
		Jura and Kleinmann (1989)
	(K-[12], [12]-[25]) Color-Color Diagram	Suh and Hong (2017)
		Epchtein et al. (1987)
IRTS	([2.30–3.77], [2.20–2.30]) Color-Color Diagram	Le Bertre et al. (2001)
		Le Bertre et al. (2003)
		IRTS Team et al. (1997)
SDSS	(g-r, g-i) Color-Color Diagram	Hill et al. (2024)

The (TiO CN, V i) color-color diagram based on the V and i filters is shown in Figure 7, which indicate effective temperature, and the TiO and CN filters, which distinguish between O-rich AGB and C-rich AGB characteristics (Nowotny et al., 2001). The classification criteria correspond from Equation 10–13.

$$i_0 > 18.5 \ (no\ RSGs), \tag{10}$$

$$M_{bol} < -3.5 \ (tip\ of\ RGB), \tag{11}$$

For O-rich AGB stars:

$$(V-i)_0 > 1.62, (TiO-CN)_0 > 0.15, \tag{12}$$

For C-rich AGB stars:

$$(V-i)_0 > 1.62, (TiO-CN)_0 < -0.3. \tag{13}$$

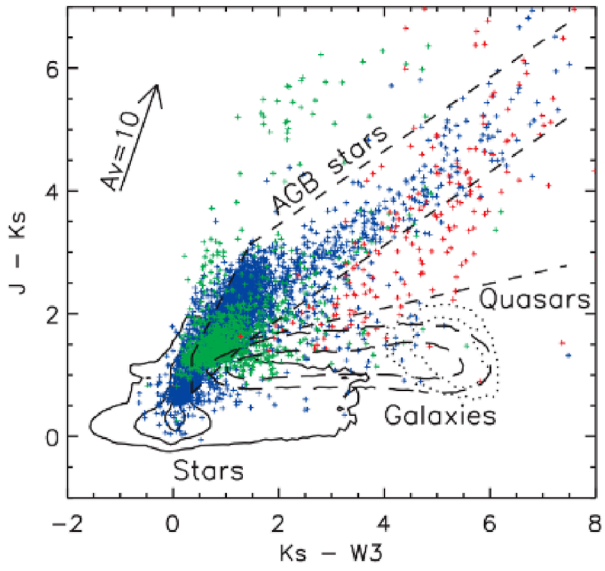

FIGURE 5
J-Ks *versus* Ks-W3 color-color diagram of the known C-rich and O-rich stars (blue: C-rich AGB stars; green: AGB stars; red: O-rich stars). Picture reproduced from Waters et al. (1999) with permission from © RAA.

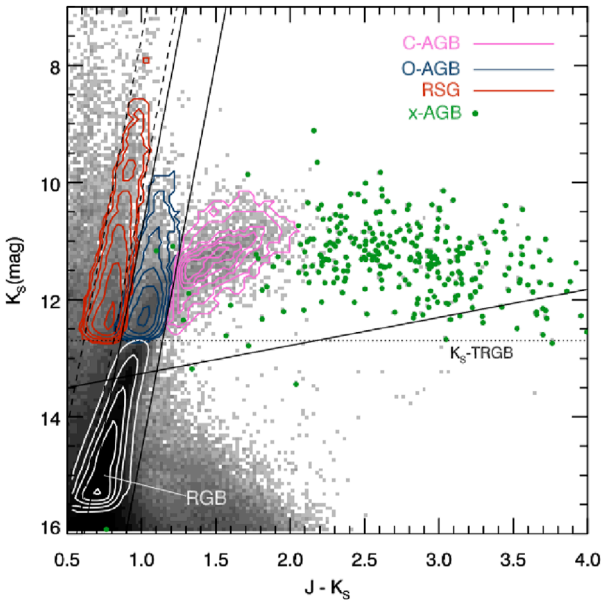

FIGURE 6
J - K_s vs. K_s color-magnitude diagram showing the separation of carbon-rich and oxygen-rich AGB stars in the Small Magellanic Cloud, with the selection of C-rich AGB (pink), O-rich AGB (blue), RSG (red),and RGB (white) stars shown in contours. The x-AGB stars (heavily extinguished "extreme" stars with a thick dust envelope), are also plotted in green. Picture reproduced from Boyer et al. (2011) by permission of the AAS.

3.2 Search methods based on light curves

Since E-AGB stars have not exhibited obvious variability characteristics in studies to date, they cannot yet be detected through light curves. However, TP-AGB stars typically exhibit various forms of variability: many are Long Period Variables (LPVs) with large amplitude variations, known as Mira variables, while others show semiregular or irregular pulsations. The large-amplitude variations characteristic of Mira variables allow TP-AGB star samples to be identified from variable star catalogs based on light curve amplitude criteria (Matsunaga et al., 2009; Bhardwaj et al., 2019; Schultheis et al., 2020; Lee et al., 2021). For instance, in the Catalina Southern Survey (CSS) catalog of LPVs, stars with light curve amplitudes ΔmCSS >0.45 mag and obeying $(m_{CSS} - K_s) > 2.0$ were identified as TP-AGB stars (Mauron et al., 2021). In the Gaia DR3 long-period variable candidate catalogue (Lebzelter et al., 2023), Sanders and Matsunaga (2023) selected all LPVs with peak-to-peak semi-amplitudes larger than 0.32 mag in Gaia G band as AGB stars.

3.3 Search methods based on infrared spectra

Currently, the search for AGB stars based on infrared spectroscopy primarily revolves around infrared spectral data from IRAS and ISO (Kwok et al., 1997; Sylvester et al., 1999; Waters et al., 1999; Wright et al., 2009; Groenewegen and Sloan, 2018; Suh, 2021). The IRAS Low-Resolution Spectrometer (LRS) (λ = 8–22 μm) data and ISO (λ = 2.4–197 μm) data are very useful for identifying important dust features of AGB stars. These features include silicate emission or absorption at 10 μm and 18 μm for O-rich AGB stars, and the silicon carbide emission feature at 11.3 μm for C-rich AGB stars. The infrared spectra of AGB stars reveal significant variations in dust features, which are related to their mass loss rates. For example, O-rich AGB stars with higher mass loss rates typically show deeper silicate absorption at 10 μm (as shown in Figure 4). Several studies have made use of these prominent infrared spectral features to identify AGB stars and investigate their infrared characteristics. Waters et al. (1999) analyzed the dust features in the infrared spectra of O-rich AGB stars using ISO data. Kwok et al. (1997) used IRAS LRS data and visually inspected the dust features of AGB stars, identifying new O-rich AGB and C-rich AGB stars from 11,224 IRAS sources.

3.4 Search methods based on radio masers

Masers (Microwave Amplification by Stimulated Emission of Radiation) occur in the outer atmosphere of AGB stars, particularly near the circumstellar envelope. Examples include SiO, H_2O, OH, HCN and SiS masers. The search methods are divided into two types. One is blind searches, where all stars in a specified region of the sky are checked for maser emission. The other is targeted searches, which use cataloged right ascension and declination data of cold giant stars obtained from previous surveys or databases. These positional data serve as the basis for the detection of maser emission from cold giant stars. Maser radiation appears as narrow and intense spectral lines, distinct from thermal emission from other astrophysical sources. Radio interferometry provides high-resolution imaging that enables precise astrometric and kinematic measurements of AGB masers (e.g., Baud et al., 1981; te Lintel Hekkert et al., 1991; Messineo et al., 2002; 2004; 2018; Kim et al., 2014).

4 Machine-learning-based methods for searching AGB stars

Identifying AGB stars in large volumes of observational data is a complex task, and traditional methods relying on manually constructed features face limitations in both efficiency and accuracy. The introduction of machine learning techniques can significantly enhance the speed and precision of AGB star identification. Currently, machine learning-based methods have been primarily applied to identify specific AGB star subtypes: S-type stars and carbon stars. For the majority of oxygen-rich AGB stars (M-type stars), due to their relatively indistinct characteristics, they are easily confused with stars in adjacent evolutionary stages (especially oxygen-rich red giants). Therefore, effective machine learning-based methods for specifically targeting this most common type of AGB star are still lacking. Given these constraints, the following sections will focus on the two AGB subtypes where machine learning approaches have shown practical success: the identification of S-type stars and C-rich AGB stars in detail.

4.1 Search methods for S-type stars based on machine learning

The methods for searching S-type stars have undergone significant historical development across different techniques. In the past, researchers have used spectra to identify S-type stars through visual inspection, initially focusing on ZrO spectral bands (Henize, 1960) and later utilizing LaO molecular features (Stephenson, 1990). In recent years, the application of machine learning in the search for S-type stars has achieved remarkable success, particularly in handling large-scale astronomical datasets. The emergence of large-scale spectroscopic survey projects has also provided more spectral data for the search of S-type star samples.

The machine learning-based search for S-type stars currently has two main papers (Chen et al., 2022; 2023). In the first paper, Chen et al. (2022) conduct a search for S-type stars using spectral data from LAMOST DR9. In the second paper, Chen et al. (2023) classify the S-type star sample into intrinsic and extrinsic S-type stars based on multiband photometric data. Below is an introduction to each of these two papers.

In the first paper, Chen et al. (2022) initially filtered the low-temperature giant samples using a color-magnitude diagram (as shown in Figure 8). The red dashed lines represent the criteria defined by Equations 14, 15:

$$M_G > 5 \cdot \frac{(G_{BP} - G_{RP})}{9} - 1, \tag{14}$$

$$G_{BP} - G_{RP} \geq 1.6, \tag{15}$$

where G_{BP} and G_{RP} are the Gaia blue and red band magnitudes, respectively.

Then, they calculated the ZrO band strength B_{ZrO} for S-type and M-type giant stars, using the criterion $B_{ZrO} > 0.25$ to preliminarily distinguish between S-type and M giants. This criterion was applied to the spectra of low-temperature

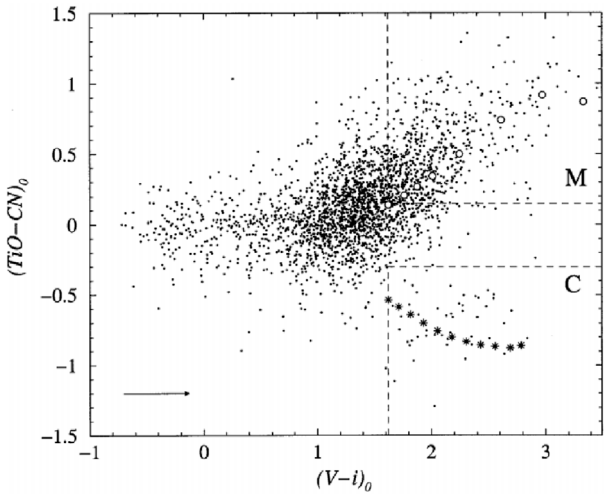

FIGURE 7
Color-color diagram and the selection areas for O-rich and C-rich stars. Synthetic photometry is plotted as well (M-stars with open circles, C-stars with asterisks). Credit: Nowotny et al. (2001), A&A, 367, 557, reproduced with permission © ESO.

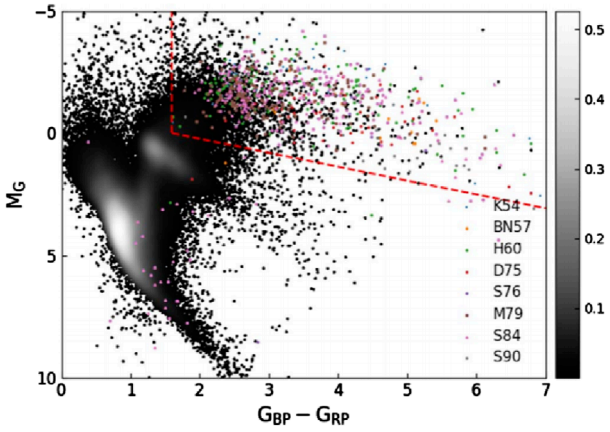

FIGURE 8
Location of the sample of low-temperature giants in the Hertzsprung-Russell diagram, from Chen et al. (2022). The dots with different colors denote the known S-type stars, and the red dashed lines indicate the criterion for selecting the low-temperature-giant sample. The color-coded density distribution represents the background stars.

giant stars. The band strength index was calculated using Equation 16:

$$B_{ZrO} = 1 - \frac{\lambda_{C,f} - \lambda_{C,i}}{\lambda_{B,f} - \lambda_{B,i}} \cdot \frac{\int_{\lambda_{B,i}}^{\lambda_{B,f}} F_\lambda \, d\lambda}{\int_{\lambda_{C,i}}^{\lambda_{C,f}} F_\lambda \, d\lambda}. \tag{16}$$

where F_λ is the observed flux within the wavelength range $(\lambda, \lambda + d\lambda)$, $\lambda_{C,f} - \lambda_{C,i}$ is the continuum window, $\lambda_{B,f} - \lambda_{B,i}$ is the ZrO molecular band window, and their definitions are listed in Table 2.

After the above steps, a sample of S-type star candidates was obtained, and then the authors used the SVM algorithm to

TABLE 2 Boundaries of the continuum and ZrO molecular band window used in the computation of the band indices (Chen et al., 2022).

Band	$\lambda_{B,i}$	$\lambda_{B,f}$	$\lambda_{C,i}$	$\lambda_{C,f}$
ZrO_1	6345.0	6352.0	6464.0	6472.0
ZrO_2	6378.0	6382.0	6464.0	6472.0
ZrO_3	6474.0	6479.0	6464.0	6472.0
ZrO_4	6508.0	6512.0	6464.0	6472.0

further distinguish S-type stars from non-S-type stars among the obtained candidates. The input features were four ZrO bands with specific wavelengths listed in Table 2. Subsequently, the authors used absolute bolometric magnitudes to further distinguish between S-type stars and red supergiant stars (RSGs) to obtain a reliable set of S-type stars. The reliability of the classification results was verified by the stars' positions on the color-magnitude diagram and their C/O ratios.

In subsequent research, Chen et al. (2023) further utilized LAMOST DR10 data, combining the XGBoost algorithm with traditional color-color diagrams to classify S-type stars into intrinsic and extrinsic types, achieving a classification accuracy of around 95%. Through feature importance ranking in XGBoost, the study also found that spectral features such as Zr I (6451.6 Å), Ne II (6539.6 Å), Hα (6564.5 Å), Fe I (6609.1 Å), and C I (6611.4 Å) play a critical role in distinguishing intrinsic and extrinsic types of S-type stars.

The application of these machine learning methods significantly improved the efficiency and accuracy of S-type star identification, providing valuable scientific insights into the evolution of AGB stars.

4.2 Search methods for carbon stars based on machine learning

Traditionally, the search for carbon stars is mainly carried out through feature engineering (manual extraction of features) for preliminary selection and linear division, followed by visual inspection. The extracted features primarily include the.

Molecular band indices of C_2 and CN, light curve characteristics, and color and luminosity features (Christlieb et al., 2001; Margon et al., 2002; Downes et al., 2004; Ji et al., 2016; Lebzelter et al., 2023; Li et al., 2024).

With the increasing volume of spectra from large-scale surveys, traditional methods that rely on linear division techniques using band indices and other extracted features have proven insufficient in terms of efficiency and accuracy, often missing many carbon star spectra. To improve the effectiveness of carbon star searches, subsequent studies have increasingly utilized more efficient machine learning algorithms.

Si et al. (2014) used observed spectra and continuum-subtracted spectra as features, which were fused through graph construction with adjacency matrices, and applied the label propagation algorithm to search for carbon stars from SDSS DR8 spectral survey, achieving recall rates larger than 0.9 and finding 260 new carbon stars. Si et al. (2015) improved upon the work of Si et al. (2014) by enhancing the graph construction method for input features and replacing the core algorithm with the efficient manifold ranking (EMR) method. This approach achieved recall rates similar to those of Si et al. (2014) while improving computational speed by approximately 55 times, and ultimately discovered 158 new carbon stars from the LAMOST pilot survey. Li et al. (2018) applied the Bagging TopPush algorithm, using preprocessed carbon star spectra from LAMOST and SDSS as positive samples, to identify 1,415 new carbon stars in the LAMOST DR4. Roulston et al. (2025) inputted Gaia colors, Gaia XP spectral coefficients and spectral indices from Gaia XP spectra into supervised classifiers (XGBoost and Random Forest), identifying 43,574 candidate carbon stars.

Traditional machine learning methods for carbon star search require experienced experts to spend a lot of time on feature engineering, which plays a crucial role in machine learning. In contrast, deep learning is an end-to-end approach that reduces the reliance on manually constructed features. As the sample size of carbon stars increases, deep learning algorithms have also been introduced to carbon star searches.

Ye et al. (2025) propose a classification model named 'GaiaNet', an improved one-dimensional convolutional neural network specifically designed for handling Gaia's XP spectra, and obtained 451 new candidate carbon stars. In this study, the SHAP interpretability method was utilized to enhance the interpretability of spectral features.

He et al. (2024) proposed a five-class deep learning model based on convolutional neural networks (CNN) to analyze LAMOST DR9 data, whose structure is shown in Figure 9, successfully identifying 4,383 carbon stars, of which 1,197 were newly discovered. The model achieved a precision of 99.45% and a recall of 91.21% for carbon star identification, providing a new technological support for the automated classification of carbon stars.

In summary, with the continuous development of machine learning algorithms, from traditional spectral indices and linear division to machine learning models and deep learning models, the efficiency and accuracy of carbon star identification have been significantly improved. These studies provide important references for large-scale data processing of carbon stars in astronomy and offer well-prepared samples to further understand the properties and evolution of carbon stars.

5 Challenges and prospects

In the search for AGB stars, although machine learning and deep learning techniques have been introduced in recent years, significant challenges remain in handling complex observational data and achieving accurate identification. With the increasing volume of observational data and growing identification requirements, overcoming current technical bottlenecks and fully utilizing advanced algorithmic approaches have become key to enhancing the efficiency and accuracy of AGB star searches. This section will explore in detail the challenges and future directions in the search for AGB stars, with the aim of providing reference and inspiration for future research.

(1) Limitation of Data Sample Size and Algorithm Selection. Due to the scarcity of observational data on AGB stars, selecting an appropriate algorithm poses a major challenge. Deep learning models have an advantage in recognizing subtle differences in

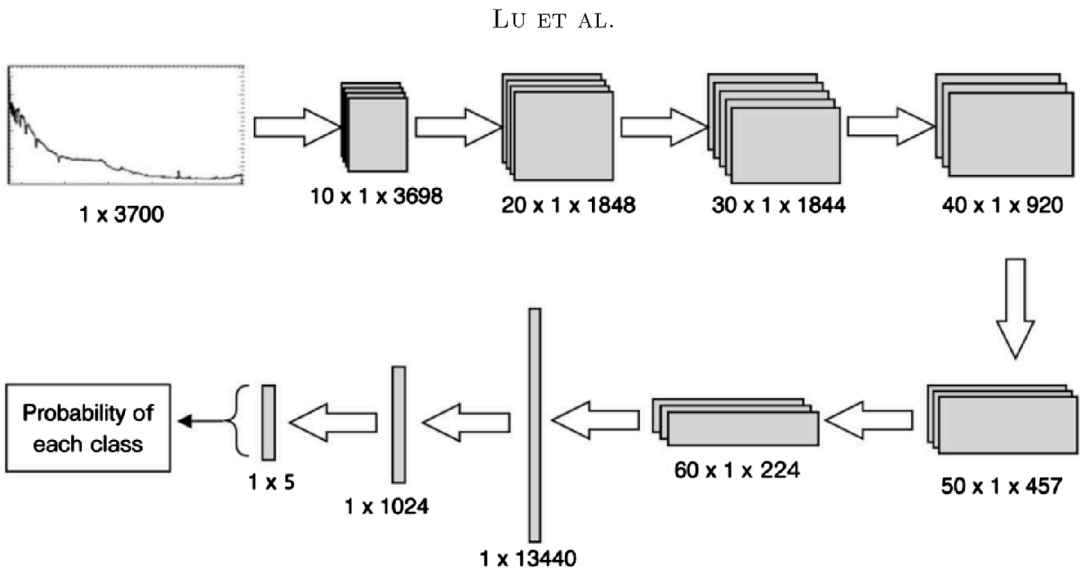

FIGURE 9
The convolutional neural network-based model architecture proposed by He et al. (2024) for classifying five subtypes of carbon stars.

features, but they require a large amount of data. However, observational data on AGB stars are often scarce and difficult to obtain. In such cases, traditional feature engineering or machine learning methods may be more advantageous when working with limited samples. Therefore, future research should choose suitable algorithms based on specific data volume and feature requirements to improve identification accuracy and efficiency.

(2) Imbalanced Sample Problem. The scarcity of AGB star observational data, especially the imbalance between positive and negative samples, can affect the training performance of models. In the future, generative models (e.g., autoencoders and diffusion models) can be used to generate synthetic samples to compensate for the lack of real data. Balancing and generating samples is one of the key directions for improving the recognition performance of machine learning models.

(3) Multi-modal Data Fusion. The fusion of multi-modal data and the construction of multi-modal models for AGB stars is also a future research direction. By integrating multi-band observational data, researchers can more comprehensively characterize the physical properties of AGB stars. Using multi-modal data fusion techniques, such as contrastive learning methods or cross-modal attention mechanisms, can achieve effective integration of multiple data sources, thereby improving classification accuracy and model generalization ability. This provides an important direction for future research in the search for AGB stars.

(4) Challenges in Algorithm Interpretability. Current deep learning algorithms can achieve good classification results, but their "black box" nature makes them difficult for scientists to accept. To address this issue, future research can introduce interpretability tools such as SHAP to reveal the model's focus on specific features and improve algorithm interpretability. For example, applying interpretative analysis to models like XGBoost, SVM, and CNN can help understand the influence of different spectral features on AGB star classification, thereby optimizing the feature selection process and enhancing the overall performance and interpretability of the model. This is also significant for theoretical validation and feature discovery in scientific research.

In conclusion, research on AGB star searches is gradually shifting from traditional methods to those based on machine learning and deep learning. In the future, with the collaborative application of various methods such as multi-modal data fusion, generative models, and interpretability tools, the identification and classification of AGB stars are expected to achieve higher precision and efficiency. This will not only enrich the AGB star sample library but also provide more solid data support for stellar evolution and cosmological research.

6 Conclusion

The search methods for AGB (Asymptotic Giant Branch) stars have evolved from traditional manual feature engineering and visual inspection to the gradual development of modern machine learning approaches. Early searches primarily relied on astronomers' expertise to identify AGB stars based on their spectral features, photometry data and variability characteristics. However, with the increase in observational data and the application of multi-wavelength techniques such as infrared and radio, researchers have progressively incorporated more diverse observational methods, such as using enhanced infrared emission and maser radiation characteristics for detection. In recent years, machine learning and deep learning-based methods have become mainstream, significantly improving the efficiency and accuracy of AGB star searches.

Nevertheless, the search for AGB stars still faces numerous challenges. First, observational data are sparse and unevenly distributed, with a substantial imbalance between positive and negative samples, which poses difficulties for training machine learning models. Additionally, the "black box" nature of current deep learning models limits their widespread application in

scientific research, as scientists find it challenging to understand the basis of the models' decisions.

In the future, with the accumulation of observational data and the application of new technologies, the search and identification of AGB stars are expected to enter a new phase. The application of generative models, interpretability tools, and multimodal data fusion will further enhance the accuracy of AGB star identification and the interpretability of models. By integrating multi-wavelength data, scientists will be able to more comprehensively characterize the physical properties of AGB stars, providing robust theoretical and data support for stellar evolution and cosmological research. The field of AGB star searches will continue to achieve breakthroughs in both precision and efficiency, offering valuable insights into the late evolutionary processes of stars and the cycle of interstellar matter.

Author contributions

H-LL: Writing – original draft, Writing – review and editing. Y-BL: Writing – review and editing. A-LL: Resources, Writing – review and editing. Z-QZ: Writing – review and editing. X-MK: Writing – review and editing. Z-PY: Writing – review and editing. HJ: Writing – review and editing, Validation, Investigation. J-CL: Formal Analysis, Software, Writing – review and editing. SL: Formal Analysis, Software, Writing – review and editing.

Funding

The author(s) declare that financial support was received for the research and/or publication of this article. This work is supported by the National Natural Science Foundation of China (12273078, 12411530071, 12273075, 12473104, 12261141689), National Astronomical Observatories of the Chinese Academy of Sciences (No. E4ZR0516), and the Royal Society (IEC/NSFC/233140).

Conflict of interest

The authors declare that the research was conducted in the absence of any commercial or financial relationships that could be construed as a potential conflict of interest.

Generative AI statement

The author(s) declare that Generative AI was used in the creation of this manuscript. Solely for literature search and language polishing.

Publisher's note

References

Albert, L., Demers, S., and Kunkel, W. E. (2000). A carbon star survey of the local group dwarf galaxies. I. IC 1613. *AJ* 119 (6), 2780–2788. doi:10.1086/301387

Battinelli, P., and Demers, S. (2011). "The elusive AGB population in galaxies,". *Why galaxies Care about AGB stars II: shining Examples and common inhabitants, volume 445 of astronomical Society of the pacific conference series*. Editors F. Kerschbaum, T. Lebzelter, and R. F. Wing, 479.

Baud, B., Habing, H. J., Matthews, H. E., and Winnberg, A. (1979). A systematic search at 1612 MHz for OH maser sources. I. Survey near the Galactic Centre. *A&AS* 35, 179–192.

Baud, B., Habing, H. J., Matthews, H. E., and Winnberg, A. (1981). A systematic search at 1612 MHz for OH maser sources. *A&A* 95, 156–170.

Bhardwaj, A., Kanbur, S., He, S., Rejkuba, M., Matsunaga, N., de Grijs, R., et al. (2019). Multiwavelength Period-luminosity and period-luminosity-color relations at maximum light for Mira variables in the magellanic clouds. *ApJ* 884 (1), 20. doi:10.3847/1538-4357/ab38c2

Blum, R. D., Mould, J. R., Olsen, K. A., Frogel, J. A., Werner, M., Meixner, M., et al. (2006). Spitzer SAGE survey of the large magellanic Cloud. II. Evolved stars and infrared color-magnitude diagrams. *AJ* 132 (5), 2034–2045. doi:10.1086/508227

Boyer, M. L., Srinivasan, S., van Loon, J. T., McDonald, I., Meixner, M., Zaritsky, D., et al. (2011). Surveying the agents of galaxy evolution in the tidally stripped, low metallicity small magellanic Cloud (SAGE-SMC). II. Cool evolved stars. *AJ* 142 (4), 103. doi:10.1088/0004-6256/142/4/103

Brewer, J. P., Richer, H. B., and Crabtree, D. R. (1995). Late-type stars in M31. I. Photometric study of AGB stars and metallicity gradients. *AJ* 109, 2480. doi:10.1086/117466

Campbell, S. W., D'Orazi, V., Yong, D., Constantino, T. N., Lattanzio, J. C., Stancliffe, R. J., et al. (2013). Sodium content as a predictor of the advanced evolution of globular cluster stars. *Nature* 498 (7453), 198–200. doi:10.1038/nature12191

Chen, J., Li, Y.-B., Luo, A. L., Ma, X.-X., and Li, S. (2023). S-Type stars from LAMOST DR10: classification of intrinsic and extrinsic stars. *ApJS* 267 (1), 5. doi:10.3847/1538-4365/acd05b

Chen, J., Luo, A. L., Li, Y.-B., Chen, X.-L., Wang, R., Li, S., et al. (2022). S-Type stars discovered in medium-resolution spectra of LAMOST DR9. *ApJ* 931 (2), 133. doi:10.3847/1538-4357/ac66de

Christlieb, N., Green, P. J., Wisotzki, L., and Reimers, D. (2001). The stellar content of the Hamburg/ESO survey II. A large, homogeneously-selected sample of high latitude carbon stars. *A&A* 375, 366–374. doi:10.1051/0004-6361:20010814

Cioni, M. R. L., Girardi, L., Marigo, P., and Habing, H. J. (2006a). AGB stars in the Magellanic Clouds. II. The rate of star formation across the LMC. *A&A* 448 (1), 77–91. doi:10.1051/0004-6361:20053933

Cioni, M. R. L., Girardi, L., Marigo, P., and Habing, H. J. (2006b). AGB stars in the magellanic clouds. III. The rate of star formation across the small magellanic Cloud. *A&A* 452 (1), 195–201. doi:10.1051/0004-6361:20054699

Cioni, M. R. L., and Habing, H. J. (2003). AGB stars in the Magellanic Clouds. I. The C/M ratio. *A&A* 402, 133–140. doi:10.1051/0004-6361:20030226

Cristallo, S., Straniero, O., Gallino, R., Piersanti, L., Domínguez, I., and Lederer, M. T. (2009). Evolution, nucleosynthesis, and yields of low-mass asymptotic giant branch stars at different metallicities. *ApJ* 696 (1), 797–820. doi:10.1088/0004-637X/696/1/797

Cutri, R. M., Skrutskie, M. F., van Dyk, S., Beichman, C. A., Carpenter, J. M., Chester, T., et al. (2003). *2MASS all sky catalog of point sources*. NASA/IPAC Infrared Science Archive.

Deacon, R. M., Chapman, J. M., Green, A. J., and Sevenster, M. N. (2007). H_2O maser observations of candidate post-AGB stars and discovery of three high-velocity water sources. *ApJ* 658 (2), 1096–1113. doi:10.1086/511383

Downes, R. A., Margon, B., Anderson, S. F., Harris, H. C., Knapp, G. R., Schroeder, J., et al. (2004). Faint high-latitude carbon stars discovered by the sloan digital sky survey: an initial catalog. *AJ* 127 (5), 2838–2849. doi:10.1086/383211

Engels, D. (2005). Agb and post-agb stars. Available online at: https://arxiv.org/abs/astro-ph/0508285.

Engels, D., and Bunzel, F. (2015). A database of circumstellar OH masers. *A&A* 582, A68. doi:10.1051/0004-6361/201322589

Epchtein, N., Le Bertre, T., Lepine, J. R. D., Marques Dos Santos, P., Matsuura, O. T., and Picazzio, E. (1987). Valinhos 2.2 micron survey of the southern galactic plane.II. Near-IR photometry, IRAS identifications and nature of the sources. *A&AS* 71, 39–55.

Feng, Y., Li, X., Yang, X., Millar, T. J., Szczerba, R., Qin, S.-L., et al. (2024). Observations of molecular CN toward S-type asymptotic giant branch stars. *AJ* 168 (6), 285. doi:10.3847/1538-3881/ad8ba6

Fonfría Expósito, J. P., Agúndez, M., Tercero, B., Pardo, J. R., and Cernicharo, J. (2006). High-J v=0 SiS maser emission in irc +10216: a new case of infrared overlaps. *ApJL* 646 (2), L127–L130. doi:10.1086/507104

Gobrecht, D., Cristallo, S., Piersanti, L., and Bromley, S. T. (2017). Nucleation of small silicon carbide dust clusters in AGB stars. *ApJ* 840 (2), 117. doi:10.3847/1538-4357/aa6db0

Goldman, S. R., Boyer, M. L., Dalcanton, J., McDonald, I., Girardi, L., Williams, B. F., et al. (2022). A census of thermally pulsing AGB stars in the andromeda galaxy and a first estimate of their contribution to the global dust budget. *ApJS* 259 (2), 41. doi:10.3847/1538-4365/ac4d9e

Gray, R. O., and Corbally, C. J. (2009). *Stellar spectral classification*. Princeton, NJ: Princeton University Press.

Groenewegen, M. A. T., Lançon, A., and Marescaux, M. (2009). Near-infrared spectroscopy of AGB star candidates in Fornax, Sculptor, and NGC 6822. *A A* 504 (3), 1031–1040. doi:10.1051/0004-6361/200911675

Groenewegen, M. A. T., and Sloan, G. C. (2018). Luminosities and mass-loss rates of Local Group AGB stars and red supergiants. *A&A* 609, A114. doi:10.1051/0004-6361/201731089

Gruyters, P., Casagrande, L., Milone, A. P., Hodgkin, S. T., Serenelli, A., and Feltzing, S. (2017). First evidence of multiple populations along the AGB from Strömgren photometry. *A&A* 603, A37. doi:10.1051/0004-6361/201630341

Habing, H. J., and Olofsson, H. (2004). "Asymptotic giant branch stars," in *Astronomy and astrophysics library*. Springer. doi:10.1007/978-1-4757-3876-6

He, Y., Cao, Z., Deng, H., Wang, F., Mei, Y., and Tan, L. (2024). Identification of carbon stars in LAMOST DR9 based on deep learning. *ApJS* 274 (1), 6. doi:10.3847/1538-4365/ad6261

Henize, K. G. (1960). S stars south of declination -25deg. *AJ* 65, 491. doi:10.1086/108296

Herwig, F. (2005). Evolution of asymptotic giant branch stars. *ARA&A* 43 (1), 435–479. doi:10.1146/annurev.astro.43.072103.150600

Hill, L., Maraston, C., Thomas, D., Yan, R., Chen, Y., Stringfellow, G. S., et al. (2024). Carbon- and Oxygen-rich stars in MaStar: identification and classification. *MNRAS* 530 (2), 1534–1549. doi:10.1093/mnras/stae919

Höfner, S., and Olofsson, H. (2018). Mass loss of stars on the asymptotic giant branch. Mechanisms, models and measurements. *A&A* 26 (1), 1. doi:10.1007/s00159-017-0106-5

Iben, J., and Renzini, A. (1983). Asymptotic giant branch evolution and beyond. *ARA&A* 21, 271–342. doi:10.1146/annurev.aa.21.090183.001415

Ivezić, Ž., and Knapp, G. R. (1999). "Link between mass-loss and variability type for agb stars?," in *Asymptotic giant Branch stars, IAU symposium 191, volume 191 of IAU symposium*. Editors T. Le Bertre, A. Lebre, and C. Waelkens (San Francisco: Astronomical Society of the Pacific), 395. doi:10.48550/arXiv.astro-ph/9812421

Jayasinghe, T., Stanek, K. Z., Kochanek, C. S., Shappee, B. J., Holoien, T. W. S., Thompson, T. A., et al. (2019). The ASAS-SN catalogue of variable stars - II. Uniform classification of 412 000 known variables. *MNRAS* 486 (2), 1907–1943. doi:10.1093/mnras/stz844

Ji, W., Cui, W., Liu, C., Luo, A., Zhao, G., and Zhang, B. (2016). Carbon stars from LAMOST DR2 data. *ApJS* 226 (1), 1. doi:10.3847/0067-0049/226/1/1

Jura, M., and Kleinmann, S. G. (1989). Dust-enshrouded asymptotic giant branch stars in the solar neighborhood. *ApJ* 341, 359. doi:10.1086/167499

Kacharov, N., Rejkuba, M., and Cioni, M. R. L. (2012). Spectra probing the number ratio of C- to M-type AGB stars in the NGC 6822 galaxy. *A&A* 537, A108. doi:10.1051/0004-6361/201117383

Karakas, A. I. (2014). Helium enrichment and carbon-star production in metal-rich populations. *MNRAS* 445 (1), 347–358. doi:10.1093/mnras/stu1727

Kastner, J. H., Thorndike, S. L., Romanczyk, P. A., Buchanan, C. L., Hrivnak, B. J., Sahai, R., et al. (2008). The large magellanic cloud's top 250: classification of the most luminous compact 8 μm sources in the large magellanic Cloud. *AJ* 136 (3), 1221–1241. doi:10.1088/0004-6256/136/3/1221

Keenan, P. C., and Boeshaar, P. C. (1980). Spectral types of S and SC stars on the revised MK system. *ApJS* 43, 379–391. doi:10.1086/190673

Khouri, T., Velilla-Prieto, L., De Beck, E., Vlemmings, W. H. T., Olofsson, H., Lankhaar, B., et al. (2019). Detection of highly excited OH towards AGB stars. A new probe of shocked gas in the extended atmospheres. *A&A* 623, L1. doi:10.1051/0004-6361/201935049

Kim, J., Cho, S.-H., and Kim, S. J. (2014). Statistical studies based on simultaneous SiO and H_2O maser surveys toward evolved stars. *AJ* 147 (1), 22. doi:10.1088/0004-6256/147/1/22

Kim, J., Cho, S.-H., Oh, C. S., and Byun, D.-Y. (2010). Simultaneous observations of SiO and H_2O masers toward known stellar SiO and H_2O maser sources. I. *ApJS* 188 (1), 209–241. doi:10.1088/0067-0049/188/1/209

Kwok, S., Volk, K., and Bidelman, W. P. (1997). Classification and identification of IRAS sources with low-resolution spectra. *ApJS* 112 (2), 557–584. doi:10.1086/313038

Lambert, D. L., Smith, V. V., Busso, M., Gallino, R., and Straniero, O. (1995). The chemical composition of red giants. IV. The neutron density at the s-process site. *ApJ* 450, 302. doi:10.1086/176141

Le Bertre, T., Matsuura, M., Winters, J. M., Murakami, H., Yamamura, I., Freund, M., et al. (2001). Galactic mass-losing AGB stars probed with the IRTS. I. *A&A* 376, 997–1010. doi:10.1051/0004-6361:20011033

Le Bertre, T., Tanaka, M., Yamamura, I., and Murakami, H. (2003). Galactic mass-losing AGB stars probed with the IRTS. II. *A&A* 403, 943–954. doi:10.1051/0004-6361:20030461

Lebzelter, T., Mowlavi, N., Lecoeur-Taibi, I., Trabucchi, M., Audard, M., García-Lario, P., et al. (2023). Gaia Data Release 3. The second Gaia catalogue of long-period variable candidates. *A&A* 674, A15. doi:10.1051/0004-6361/202244241

Lee, J.-E., Lee, S., Lee, S., Suh, K.-W., Cho, S.-H., Byun, D.-Y., et al. (2021). AGB interlopers in YSO catalogs hunted out by NEOWISE. *ApJL* 916 (2), L20. doi:10.3847/2041-8213/ac0d59

Leščinskaitė, A., Stonkutė, R., and Vansevičius, V. (2021). AGB and RGB stars in the dwarf irregular galaxy Leo A. *A&A* 647, A170. doi:10.1051/0004-6361/202037967

Lewis, M. O., Pihlström, Y. M., Sjouwerman, L. O., and Quiroga-Nuñez, L. H. (2020a). Infrared color separation between thin-shelled oxygen-rich and carbon-rich AGB stars. *ApJ* 901 (2), 98. doi:10.3847/1538-4357/abaf46

Lewis, M. O., Pihlström, Y. M., Sjouwerman, L. O., Stroh, M. C., Morris, M. R., and Collaboration, B. A. D. E. (2020b). Carbon- and oxygen-rich asymptotic giant branch (AGB) stars in the bulge asymmetries and dynamical evolution (BAaDE) survey. *ApJ* 892 (1), 52. doi:10.3847/1538-4357/ab7920

Li, L., Zhang, K., Cui, W., Shi, J., Ji, W., Huo, Z., et al. (2024). Identification of carbon stars from LAMOST DR7. *ApJS* 271 (1), 12. doi:10.3847/1538-4365/ad1881

Li, X., Millar, T. J., Heays, A. N., Walsh, C., van Dishoeck, E. F., and Cherchneff, I. (2016). Chemistry and distribution of daughter species in the circumstellar envelopes of O-rich AGB stars. *A&A* 588, A4. doi:10.1051/0004-6361/201525739

Li, X., Millar, T. J., Walsh, C., Heays, A. N., and van Dishoeck, E. F. (2014). Photodissociation and chemistry of N_2 in the circumstellar envelope of carbon-rich AGB stars. *A&A* 568, A111. doi:10.1051/0004-6361/201424076

Li, Y.-B., Luo, A. L., Du, C.-D., Zuo, F., Wang, M.-X., Zhao, G., et al. (2018). Carbon stars identified from LAMOST DR4 using machine learning. *ApJS* 234 (2), 31. doi:10.3847/1538-4365/aaa415

Lian, J., Zhu, Q., Kong, X., and He, J. (2014). Characterizing AGB stars in wide-field infrared survey explorer (WISE) bands. *A&A* 564, A84. doi:10.1051/0004-6361/201322818

Loup, C., Duc, P. A., Fouqué, P., Bertin, E., and Epchtein, N. (1998). "Denis survey of agb and tip-rgb stars in the lmc bar west and the optical center fields," in *The Impact of near-infrared sky Surveys on Galactic and extragalactic astronomy: Proceedings of the 3rd Euroconference on near-infrared surveys, meudon observatory, 19-20, 1997, volume 230 of Astrophysics and Space science library, page 115*. Editor N. Epchtein (Dordrecht; Boston, MA: Kluwer Academic Publishers). doi:10.1007/978-94-011-5026-2_15

Margon, B., Anderson, S. F., Harris, H. C., Strauss, M. A., Knapp, G. R., Fan, X., et al. (2002). Faint high-latitude carbon stars discovered by the sloan digital sky survey: methods and initial results. *AJ* 124 (3), 1651–1669. doi:10.1086/342284

Masa, E., Alcolea, J., Santander-García, M., Bujarrabal, V., Sánchez Contreras, C., and Castro-Carrizo. M 1-92, A. (2024). The death of an AGB star told by its isotopic ratios. *Galaxies* 12 (5), 63. doi:10.3390/galaxies12050063

Matsunaga, N., Kawadu, T., Nishiyama, S., Nagayama, T., Hatano, H., Tamura, M., et al. (2009). A near-infrared survey of Miras and the distance to the Galactic Centre. *MNRAS* 399 (4), 1709–1729. doi:10.1111/j.1365-2966.2009.15393.x

Matsuura, M., Barlow, M. J., Zijlstra, A. A., Whitelock, P. A., Cioni, M. R. L., Groenewegen, M. A. T., et al. (2009). The global gas and dust budget of the Large Magellanic Cloud: AGB stars and supernovae, and the impact on the ISM evolution. *MNRAS* 396 (2), 918–934. doi:10.1111/j.1365-2966.2009.14743.x

Mauron, N., Gigoyan, K. S., Kendall, T. R., and Hambleton, K. M. (2021). A search for distant, pulsating red giants in the southern halo. *A&A* 650, A146. doi:10.1051/0004-6361/201937005

Menten, K. M., Wyrowski, F., Keller, D., and Kamiński, T. (2018). Widespread HCN maser emission in carbon-rich evolved stars. *A&A* 613, A49. doi:10.1051/0004-6361/201732296

Messineo, M., Habing, H. J., Menten, K. M., Omont, A., and Sjouwerman, L. O. (2004). 86 GHz SiO maser survey of late-type stars in the inner Galaxy. II. Infrared photometry of the SiO target stars. *A&A* 418, 103–116. doi:10.1051/0004-6361:20034488

Messineo, M., Habing, H. J., Sjouwerman, L. O., Omont, A., and Menten, K. M. (2002). 86 GHz SiO maser survey of late-type stars in the Inner Galaxy. I. Observational data. *A&A* 393, 115–128. doi:10.1051/0004-6361:20021017

Messineo, M., Habing, H. J., Sjouwerman, L. O., Omont, A., and Menten, K. M. (2018). 86 GHz SiO maser survey of late-type stars in the Inner Galaxy. IV. SiO emission and infrared data for sources in the Scutum and Sagittarius-Carina arms, 20° < l < 50. *A&A*, 619:A35. doi:10.1051/0004-6361/201730717

Nikolaev, S., and Weinberg, M. D. (2000). Stellar populations in the large magellanic Cloud from 2MASS. *ApJ* 542 (2), 804–818. doi:10.1086/317048

Nowotny, W., Kerschbaum, F., Olofsson, H., and Schwarz, H. E. (2002). "The agb populations of local group galaxies," in *Observed HR Diagrams and stellar evolution, volume 274 of astronomical Society of the pacific conference series, page 472*. Editors T. Lejeune, and J. Fernandes (San Francisco: Astronomical Society of the Pacific).

Nowotny, W., Kerschbaum, F., Olofsson, H., and Schwarz, H. E. (2003). A census of AGB stars in Local Group galaxies. II. NGC 185 and NGC 147. *A&A* 403, 93–103. doi:10.1051/0004-6361:20030282

Nowotny, W., Kerschbaum, F., Schwarz, H. E., and Olofsson, H. (2001). A census of AGB stars in Local Group galaxies I. Photometry of a field in M 31. *A&A* 367, 557–565. doi:10.1051/0004-6361:20000463

Palmerini, S., La Cognata, M., Cristallo, S., and Busso, M. (2011). Deep mixing in evolved stars. I. The effect of reaction rate revisions from C to Al. *ApJ* 729 (1), 3. doi:10.1088/0004-637X/729/1/3

Ramstedt, S., Schöier, F. L., and Olofsson, H. (2011). "The mass-loss rates and molecular abundances of s-type agb stars," in *Why galaxies Care about AGB stars II: shining Examples and common inhabitants, volume 445 of astronomical Society of the pacific conference series, page 263, San Francisco, sept*. Editors F. Kerschbaum, T. Lebzelter, and R. F. Wing (Astronomical Society of the Pacific). doi:10.48550/arXiv.1011.2064

Roulston, B. R., Leonhardes-Barboza, N., Green, P. J., and Portnoi, E. (2025). Carbon stars from Gaia data release 3 and the Space density of dwarf carbon stars. *ApJ* 982 (2), 184. doi:10.3847/1538-4357/adba53

Sanders, J. L., and Matsunaga, N. (2023). Hunting for C-rich long-period variable stars in the Milky Way's bar-bulge using unsupervised classification of Gaia BP/RP spectra. *MNRAS* 521 (2), 2745–2764. doi:10.1093/mnras/stad574

Schneider, R., Valiante, R., Ventura, P., dell'Agli, F., Di Criscienzo, M., Hirashita, H., et al. (2014). Dust production rate of asymptotic giant branch stars in the Magellanic Clouds. *MNRAS* 442 (2), 1440–1450. doi:10.1093/mnras/stu861

Schultheis, M., Rojas-Arriagada, A., Cunha, K., Zoccali, M., Chiappini, C., Zasowski, G., et al. (2020). Cool stars in the Galactic center as seen by APOGEE. M giants, AGB stars, and supergiant stars and candidates. *A&A* 642, A81. doi:10.1051/0004-6361/202038327

Shetye, S., Goriely, S., Siess, L., Van Eck, S., Jorissen, A., and Van Winckel, H. (2019). Observational evidence of third dredge-up occurrence in S-type stars with initial masses around 1 $M_{\odot}$. *A&A* 625, L1. doi:10.1051/0004-6361/201935296

Si, J., Luo, A., Li, Y., Zhang, J., Wei, P., Wu, Y., et al. (2014). Search for carbon stars and DZ white dwarfs in SDSS spectra survey through machine learning. *Sci. China Phys. Mech. Astronomy* 57 (1), 176–186. doi:10.1007/s11433-013-5374-0

Si, J.-M., Li, Y.-B., Luo, A. L., Tu, L.-P., Shi, Z.-X., Zhang, J.-N., et al. (2015). Identifying Carbon stars from the LAMOST pilot survey with the efficient manifold ranking algorithm. *Res. Astronomy Astrophysics* 15 (10), 1671–1694. doi:10.1088/1674-4527/15/10/005

Sibbons, L. F., Ryan, S. G., Irwin, M., and Napiwotzki, R. (2015a). The AGB population in IC 1613 using JHK photometry. *A&A* 573, A84. doi:10.1051/0004-6361/201423982

Sibbons, L. F., Ryan, S. G., Napiwotzki, R., and Thompson, G. P. (2015b). Spectral classification of photometrically selected AGB candidates in NGC 6822. *A&A* 574, A102. doi:10.1051/0004-6361/201423981

Soszyński, I., Udalski, A., Szymański, M. K., Kubiak, M., Pietrzyński, G., Wyrzykowski, Ł., et al. (2009). The optical gravitational lensing experiment. The OGLE-III catalog of variable stars. IV. Long-Period Variables in the large magellanic Cloud. *AcA* 59 (3), 239–253. doi:10.48550/arXiv.0910.1354

Soszyński, I., Udalski, A., Szymański, M. K., Kubiak, M., Pietrzyński, G., Wyrzykowski, Ł., et al. (2013). The optical gravitational lensing experiment. The OGLE-III catalog of variable stars. XV. Long-Period Variables in the galactic bulge. *AcA* 63 (1), 21–36. doi:10.48550/arXiv.1304.2787

Spano, M., Mowlavi, N., Eyer, L., Burki, G., Marquette, J. B., Lecoeur-Taïbi, I., et al. (2011). Long period variables in the large magellanic Cloud from the EROS-2 survey. *A&A* 536, A60. doi:10.1051/0004-6361/201117302

Srinivasan, S., Meixner, M., Leitherer, C., Vijh, U., Volk, K., Blum, R. D., et al. (2009). The mass loss return from evolved stars to the large magellanic Cloud: empirical relations for excess emission at 8 and 24 μm. *AJ* 137 (6), 4810–4823. doi:10.1088/0004-6256/137/6/4810

Stancliffe, R. J., Tout, C. A., and Pols, O. R. (2004). Deep dredge-up in intermediate-mass thermally pulsing asymptotic giant branch stars. *MNRAS* 352 (3), 984–992. doi:10.1111/j.1365-2966.2004.07987.x

Stephenson, C. B. (1990). New and relatively faint S stars found in the northern Milky way. *AJ* 100, 569. doi:10.1086/115540

Stroh, M. C., Pihlström, Y. M., Sjouwerman, L. O., Claussen, M. J., Morris, M. R., and Rich, M. R. (2018). Quasi-simultaneous 43 and 86 GHz SiO maser observations and potential bias in the BAaDE survey are resolved. *ApJ* 862 (2), 153. doi:10.3847/1538-4357/aaccf3

Stroh, M. C., Pihlström, Y. M., Sjouwerman, L. O., Lewis, M. O., Claussen, M. J., Morris, M. R., et al. (2019). The bulge asymmetries and dynamical evolution (BAaDE) SiO maser survey at 86 GHz with ALMA. *ApJS* 244 (2), 25. doi:10.3847/1538-4365/ab3c35

Suh, K.-W. (2021). A new catalog of asymptotic giant branch stars in our galaxy. *ApJS* 256 (2), 43. doi:10.3847/1538-4365/ac1274

Suh, K.-W., and Hong, J. (2017). A new catalog of AGB stars based on infrared two-color diagrams. *J. Korean Astronomical Soc.* 50 (4), 131–138. doi:10.5303/JKAS.2017.50.4.131

Sylvester, R. J., Kemper, F., Barlow, M. J., de Jong, T., Waters, L. B. F. M., Tielens, A. G. G. M., et al. (1999). 2.4-197 mu m spectroscopy of OH/IR stars: the IR characteristics of circumstellar dust in O-rich environments. *A&A* 352, 587–599. doi:10.48550/arXiv.astro-ph/9910368

te Lintel Hekkert, P., Caswell, J. L., Habing, H. J., Haynes, R. F., Haynes, R. F., and Norris, R. P. (1991). 1612 MHz OH survey of IRAS point sources. I. Observations made at Dwingloo, Effelsberg and Parkes. *A&AS* 90, 327.

Tu, X., and Wang, Z.-X. (2013). Classification study of WISE infrared sources: identification of candidate asymptotic giant branch stars. *Res. Astronomy Astrophysics* 13 (3), 323–333. doi:10.1088/1674-4527/13/3/007

Tuo, J., Li, X., Sun, J., Millar, T. J., Zhang, Y., Qiu, J., et al. (2024). A λ 3 mm line survey toward the circumstellar envelope of the carbon-rich AGB star IRC+10216 (CW leo). *ApJS* 271 (2), 45. doi:10.3847/1538-4365/ad2460

van der Veen, W. E. C. J., and Habing, H. J. (1988). The IRAS two-colour diagram as a tool for studying late stages of stellar evolution. *A&A* 194, 125–134.

Van Eck, S., Neyskens, P., Jorissen, A., Plez, B., Edvardsson, B., Eriksson, K., et al. (2017). A grid of MARCS model atmospheres for late-type stars. II. S stars and their properties. *A&A* 601, A10. doi:10.1051/0004-6361/201525886

Vassiliadis, E., and Wood, P. R. (1993). Evolution of low- and intermediate-mass stars to the end of the asymptotic giant branch with mass loss. *ApJ* 413, 641. doi:10.1086/173033

Waters, L. B. F. M., Beintema, D. A., Cami, J., de Graauw, T., Hony, S., de Jong, T., et al. (1999). "Iso observations of agb and post-agb stars," in *The Universe as Seen by ISO, volume 427 of ESA Special Publication, page 219*. Editors P. Cox, and M. F. Kessler (Noordwijk, Netherlands: European Space Agency).

Willson, L. A. (2000). Mass loss from cool stars: impact on the evolution of stars and stellar populations. *ARA&A* 38, 573–611. doi:10.1146/annurev.astro.38.1.573

Wiśniewski, M., Marquette, J. B., Beaulieu, J. P., Schwarzenberg-Czerny, A., Tisserand, P., and Lesquoy, É. (2011). Oxygen- and carbon-rich variable red giant populations in the Magellanic Clouds from EROS, OGLE, MACHO, and 2MASS photometry. *A&A* 530, A8. doi:10.1051/0004-6361/201014319

Wright, E. L., Eisenhardt, P. R. M., Mainzer, A. K., Ressler, M. E., Cutri, R. M., Jarrett, T., et al. (2010). The wide-field infrared survey explorer (WISE): mission description and initial on-orbit performance. *AJ* 140 (6), 1868–1881. doi:10.1088/0004-6256/140/6/1868

Wright, N. J., Barlow, M. J., Greimel, R., Drew, J. E., Matsuura, M., Unruh, Y. C., et al. (2009). Near-IR spectra of IPHAS extremely red Galactic AGB stars. *MNRAS* 400 (3), 1413–1426. doi:10.1111/j.1365-2966.2009.15536.x

Wu, Y., Zhang, B., Li, J., and Zheng, X.-W. (2022). Water-maser survey towards off-plane O-rich AGBs around the orbital plane of the Sagittarius stellar stream. *MNRAS* 516 (2), 1881–1893. doi:10.1093/mnras/stac1971

Wu, Y. W., Matsunaga, N., Burns, R. A., and Zhang, B. (2018). SiO maser survey towards off-plane O-rich AGBs around the orbital plane of the Sagittarius stellar stream. *MNRAS* 473 (3), 3325–3350. doi:10.1093/mnras/stx2450

Yamamura, I., and IRTS Team (1997). "Point source observations by the IRTS,". *Diffuse infrared Radiation and the IRTS, volume 124 of astronomical Society of the pacific conference series*. Editors H. Okuda, T. Matsumoto, and T. Rollig (Astronomical Society of the Pacific), 72.

Ye, S., Cui, W.-Y., Li, Y.-B., Luo, A. L., and Jones, H. R. A. (2025). Deep learning interpretability analysis for carbon star identification in Gaia DR3. *A&A* 697, A107. doi:10.1051/0004-6361/202449619